Available online at www.sciencedirect.com
SCIENCE DIRECT
Bioorganic & Medicinal Chemistry 14 (2006) 5230–5240
Bioorganic & Medicinal Chemistry

Anticancer thiopyrano[2,3-*d*][1,3]thiazol-2-ones with norbornane moiety. Synthesis, cytotoxicity, physico-chemical properties, and computational studies

Roman Lesyk,[a,*] Borys Zimenkovsky,[a] Dmytro Atamanyuk,[a,b] Frank Jensen,[b] Katarzyna Kieć-Kononowicz[c] and Andrzej Gzella[d]

[a]*Danylo Halytsky Lviv National Medical University, Department of Pharmaceutical, Organic and Bioorganic Chemistry, Pekarska 69, Lviv 79010, Ukraine*
[b]*University of Southern Denmark, Department of Chemistry, Campusvej 55, Odense M, DK-5230, Denmark*
[c]*Collegium Medicum of Jagiellonian University, Department of Chemical Technology and Biotechnology of Drugs, Medyczna 9, Krakow, Poland*
[d]*Karol Marcinkowski Poznan University of Medical Sciences, Department and Chair of Organic Chemistry, Grundwaldzka 6, Poznan 60-780, Poland*

Received 15 November 2005; revised 9 February 2006; accepted 31 March 2006
Available online 2 May 2006

Abstract—A series of novel 9-substituted-3,7-dithia-5-azatetracyclo[9.2.1.0^{2,10}.0^{4,8}]tetradecen-4(8)-ones-6 have been synthesized by a stereoselective hetero-Diels–Alder reaction of 5-ylidene-4-thioxo-2-thiazolidone derivatives with norbornene-2. All the compounds have been evaluated for antitumor activity in in vitro human tumor cell lines, and 10 of them possessed significant and selective cytotoxicity (MGM $\log GI_{50} \sim -4.17$ to -4.98, for individual cell lines $\log GI_{50}$ up to -8). COMPARE analyses of differential growth inhibition patterns of compounds at the GI_{50} level showed high correlations with some of the antitubulin agents. The lipophilicity of the compounds was studied by RP-TLC and found to correlate well with calculated $\log P$ values. Docking and structure–activity relationship studies produced seven QSAR models with 2 or 3 variables, with correlation coefficients $r^2 > 0.9$ and leave-one-out cross-validation correlation coefficients, $q^2 > 0.8$.

1. Introduction

Thiazolidinone derivatives represent a well-known class of patented drugs and substances at different stages of research, which possess hypoglycaemic, anti-inflammatory, choleretic, antitumor, diuretic, immunostimulant, and other activities.[1,2] Recently, attention has been paid to the antitumor activity of thiazolidinone derivatives as novel potential anticancer agents (structures **I**–**IV** at Fig. 1).[1,3–7] Their antitumor activity has been associated with activation of PPAR-γ receptors with subsequent induction of cell cycle withdrawal of preadipocytes via suppression of the transcriptional activity of the E2F/DP complex and overexpression of the PTEN protein.[8–11] Although there are numerous publications regarding the antitumor potential of PPAR-γ agonists (troglitazone, rosiglitazone, pioglitazone, and ciglitazone), which mediate apoptosis in cancer cells independently of PPAR-γ receptors. Novel pharmacological targets for thiazolidine derivatives were also identified, for example, BH_3-inhibitors[3–5] (compound **II**, Fig. 1) prevent Bcl-X_L and BH_3 domain interactions with subsequent apoptosis induction by binding to antiapoptotic protein Bcl-X_L, and 2-thioxo-4-thiazolidone derivative **III** (Fig. 1)[6] inhibit binding of tumor necrosis factor α (TNF-α) to tumor necrosis factor receptor type 1 (TNFRc-1). Furthermore, compound **IV**[7] (Fig. 1) were found to have inhibitory action on translation initiation—they perform cell cycle arrest in G1 phase via partial depletion of intercellular Ca^{2+} stores.

An analysis of the National Cancer Institute (NCI, USA) registered anticancer drugs resulted in 48 monocyclic heterocycles and 39 fused heterocyclic systems

Keywords: Thiopyrano[2,3-*d*]thiazol-2-ones; Anti-cancer in vitro screening; RP-TLC lipophilicity study; Docking; 3D-QSAR.
* Corresponding author. Tel.: +380 322755966; fax: +380 322747734; e-mail: dr_r_lesyk@org.lviv.net

0968-0896/$ - see front matter © 2006 Elsevier Ltd. All rights reserved.
doi:10.1016/j.bmc.2006.03.053

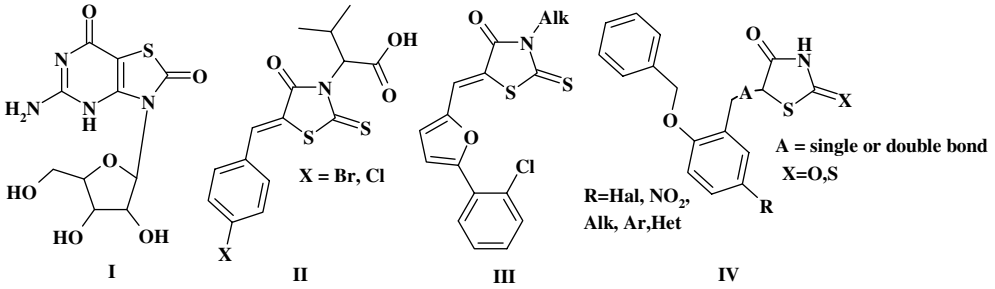

Figure 1. Structures of thiazolidine derivatives, which have potential anticancer and immunostimulant effects.

among 137 items. The NCI database contains 734 non-fused and 146 fused thiazolidine derivatives, 5 derivatives of 2-thiazolidone, 52 derivatives of thiazolidine-2-thione, and 454 derivatives of 4-thiazolidone among 42,247 compounds which have been found to be active in three tumor cell lines assay.[12] These results motivated us to search for fused thiazol-2-one derivatives as novel anticancer lead-compounds and to work on an approach for modeling the potential anticancer properties of new tetracyclic fused heterocycles. Our premise is that 4-thiazolidones are synthetic precursors of thiopyrano[2,3-*d*]thiazole group, which could imitate some pharmacologically important molecular fragments of biologically active thiazolidones. It is therefore of interest to study the influence of fusing the thiopyrane cycle and thiazolidine scaffold on the pharmacological profile of these compounds. We have paid especial attention to bioavailability features like lipophilicity, which is an important 'drug-like' property, by combining the thiopyrano[2,3-*d*]thiazole scaffold with bulky and lipophilic moiety like norbornane. Moreover the norbornane moiety could potentially bind to the lipophilic pockets of enzymes.

In the present work, we have found 10 anticancer compounds from a novel group of thiopyrano[2,3-*d*][1,3]thiazol-2-one derivatives with a norbornane fragment. Docking and QSAR studies of the compounds were performed for investigating the structure–activity relationships.

2. Chemistry

The isorhodanine (**2**) 4-thioxo- and active 5-methylene-groups create a convenient scaffold for building additional heterocyclic fragments. We have used this for synthesizing 5-ylidene-4-thioxo-2-thiazolidones (compounds **3**–**13**). The reactivity of the sulfur atom at the 4-position at 5-ylidene-4-thioxo-2-thiazolidones allows it to be used as a highly active heterodiene component in hetero-Diels–Alder reactions.[13–21] In this work, we have synthesized several new 9-substituted-3, 7-dithia-5-azatetracyclo-[9.2.1.$0^{2,10}$.$0^{4,8}$]tetradecen-4(8)-ones-6 **14**–**24** with improved lipophilic properties (Scheme 1) by coupling with norbornene-2 (bicyclo[2.2.1]heptene-2) as the dienophile.

The structures of all new compounds have been confirmed by elemental analyses, IR, ^{1}H, and ^{13}C NMR spectroscopy, and in some cases, by mass spectroscopy. The NMR spectra showed that only one stereoisomer was present for all products, indicating that the reaction is stereoselective. An X-ray crystallography was

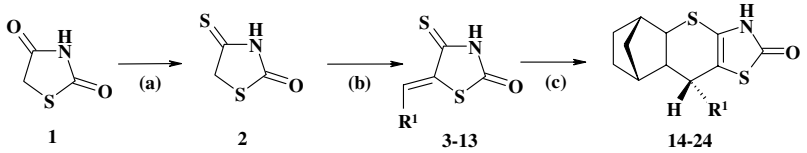

Compound	R^1
3,14	4-Cl-C_6H_4-
4,15	4-CH_3O-C_6H_4-
5,16	4-CH_3-C_6H_4-
6,17	4-HO-C_6H_4-
7,18	2-Cl-C_6H_4-
8,19	thiophen-2-yl-
9,20	3,4-$(CH_3O)_2$-C_6H_3-
10,21	4-(C_6H_5-CH_2O) -3-CH_3O-C_6H_4-
11,22	2-(2',5'-dichloro-phenyl)furan-2-yl-
12,23	4-F-C_6H_4-
13,24	4-HO-3-CH_3O-C_6H_4-

Scheme 1. Synthesis of novel 3,5,6,7-tetrahydro-2*H*-thiopyrano[2,3-*d*][1,3]thiazol-2-ones with norbornane moiety. Reagents: (a) P_2S_5, dioxane (Ref. 13); (b) R^1CHO (1.1 equiv), AcONa (1 equiv), AcOH; (c) norbornene (1.2 equiv), hydroquinone, AcOH.

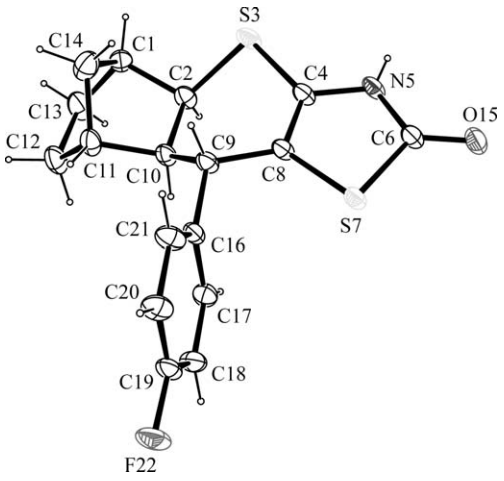

Figure 2. X-ray structure of the compound **23**.

performed on compound **23** in order to determine the exact stereoisomer. The molecular structure and atom-labeling scheme are illustrated in Figure 2. The most important aspect of the structure is the relative stereochemistry of the H atoms in the stereogenic C2, C9, and C10 centers. The H atoms at C2 and C10 have a *cis* axial–axial orientation. The H atom at C9 occupies an axial position with respect to the dihydrothiopyrane ring. The torsion angle H9–C9–C10–H10 of −163° reveals an antiperiplanar conformation for atoms H9 and H10. The phenyl ring is attached equatorially to the dihydrothiopyrane ring and is twisted 80.86(8)° relative to the mean plane. In the solid state, both five-membered carbocyclic rings (C1, C2, C10, C11, and C14; C1, C11, C12, C13, and C14) have a C14-envelope conformation {Cremer and Pople[22] puckering parameters: $Q = 0.587(4)$ Å, $\varphi = 144.2(3)°$ and $Q = 0.584(4)$ Å, $\varphi = 321.5(4)°$, respectively}, whereas the five-membered heterocyclic ring (C4, N5, C6, S7, and C8) is remarkably planar with mean deviation of 0.010 Å. The six-membered carbo- and heterocyclic rings of the polycyclic skeleton have a boat conformation distorted to different degrees {Cremer and Pople puckering parameters are $Q = 0.964(3)$ Å, $\theta = 89.3(2)°$, $\varphi = 358.6(2)°$ and $Q = 0.674(3)$ Å, $\theta = 92.6(3)°$, $\varphi = 185.6(3)°$, respectively}. The endocyclic double bond C4=C8 has a bond length of 1.338(3) Å, while the C6–N5 bond distance [1.355(4) Å] is somewhat longer than the normal length of the C_{sp^2}–N bond [1.331(2) Å] for γ-lactams.[23]

Apart from normal van der Waals interactions, the molecular packing in the crystal lattice is stabilized by N5–H···O15^{i} hydrogen bonds {N5···O15^{i} = 2.884(3) Å, H5···O15^{i} = 2.18(4) Å, N5–H5···O15^{i} = 157(4)°, (i) $1 - x, -y, -z$} linking the molecules related by inversion center into dimers.

3. Evaluation of anticancer activity in vitro

All the new thiopyrano[2,3-*d*]thiazol-2-one derivatives with norbornane moiety (**14**–**24**) were submitted and evaluated against three human tumor cell lines panel, consisting of NCI-H460 (non-small cell lung cancer), MCF7 (breast cancer), and SF-268 (CNS cancer) cell lines. Primary anticancer assays were performed according to the US NCI protocol and described elsewhere.[24–26] The substances which reduced the growth of the cell lines to 32% or less (negative numbers indicate cell kill) were passed on for evaluation in the full panel of 60 human tumor cell lines. Only compound **24** was found to be inactive in the prescreening stage, and compounds **14**–**23** were consequently selected for in vitro testing against the full panel. The human tumor cell lines subpanels were derived from nine different cancer types: leukemia, melanoma, lung, colon, CNS, ovarian, renal, prostate, and breast cancers, and used at 10-fold dilutions of five concentrations (100, 10, 1, 0.1, and 0.01 μM).[24–26] Based on the cytotoxicity assays, three antitumor activity dose–response parameters were calculated for each experimental agent against each cell line: GI_{50}—molar concentration of the compound that inhibits 50% net cell growth; TGI—molar concentration of the compound leading to total inhibition; and LC_{50}—molar concentration of the compound leading to 50% net cell death. Values were calculated for each of these parameters if the level of activity was reached; if the effect was not reached or was exceeded, the value is expressed as greater or less than the maximum or minimum concentration tested. Furthermore, a mean graph midpoints (MG_MID) were calculated for each of the parameters, giving an averaged activity parameter over all cell lines for each compound. For the calculation of the MG_MID, insensitive cell lines are included with the highest concentration tested. The results of the primary screening and the full panel screening are summarized in Table 1.

The highest average total growth inhibition and the highest mean $\log GI_{50}$ values were found for compounds **15**, **16**, **18**, **22**, and **23**, whereas compounds **14**, **15**, **17**, **18**, **21**, and **22** appeared to be most active against selected individual cell lines with the $\log GI_{50}$ varying from −8.00 to −5.49 ($GI_{50} \sim 10$–0.01 μM). Some of the most potent inhibition results of human tumor cell growth were found for compounds **15**, **16**, **18**, and **23**, and the full activity pattern against all cell lines is available as Supplementary data.

The tested compounds showed a broad spectrum of growth inhibition activity against human tumor cells, as well as some distinctive patterns of selectivity. For example, compound **14** (MG_MID $\log GI_{50} = -4.33$) appeared to be more selective against the leukemia cell lines panel ($\text{mean}_{\text{Leuk}}\ \log GI_{50} = -4.83$), compound **18** (MG_MID $\log GI_{50} = -4.83$) was more selective against renal cell lines panel ($\text{mean}_{\text{Renal}}\ \log GI_{50} = -5.02$), while compound **15** (MG_MID $\log GI_{50} = -4.98$) appeared to be more potent against non-small cell lung cancer (NSCL) ($\text{mean}_{\text{NSCL}}\ \log GI_{50} = -5.16$) and melanoma cell lines ($\text{mean}_{\text{Melanoma}}\ \log GI_{50} = -5.37$); compound **21** (MG_MID $\log GI_{50} = -4.62$)—against NSCL ($\text{mean}_{\text{NSCL}}\ \log GI_{50} = -4.74$), CNS cancer ($\text{mean}_{\text{CNS}}\ \log GI_{50} = -4.83$), and renal cancer ($\text{mean}_{\text{Renal}}\ \log GI_{50} = -5.01$); compound **22** (MG_MID $\log GI_{50} = -4.92$) was found to be a highly active

Table 1. In vitro anticancer activity for compounds **14**–**24**

Compound	NSC (NCI code)	Three cell lines assay[a]			Active[b]	N^c	$\log GI_{50}$			$\log TGI$			$\log LC_{50}$		
		A	B	C			$N1^c$	Range	MG_MID	$N2^c$	Range	MG_MID	$N3^c$	Range	MG_MID
14	731906	2	92	57	Y	51	45	−5.59 to −4.05	−4.33	8	−5.01 to −4.03	−4.04	1	−4.14	−4
15[d]	729853	3	14	6	Y	50	50	−7.54 to −4.24	−4.98	46	−5.32 to −4.09	−4.47	37	−4.38 to −4.03	−4.16
16	729726	3	45	27	Y	47	47	−4.89 to −4.39	−4.77	45	−4.77 to −4.12	−4.45	42	−4.40 to −4.02	−4.16
17	729725	1	12	2	Y	49	45	<−8.00;[d] −4.94 to −4.15	−4.61	33	−4.59 to −4.01	−4.21	16	−4.24 to −4.01	−4.04
18	729844	1	1	2	Y	49	49	−6.05 to −4.25	−4.83	44	−4.81 to −4.02	−4.45	37	−4.39 to −4.03	−4.16
19	731898	17	113	72	Y	54	30	−4.77 to −4.02	−4.17	6	−4.44 to −4.06	−4.02	1	−4.11	−4
20	731896	14	98	49	Y	51	49	−4.84 to −4.26	−4.59	35	−4.52 to −4.05	−4.23	18	−4.25 to −4.07	−4.05
21	733571	13	39	43	Y	56	50	−5.49 to −4.25	−4.62	29	−5.09 to −4.08	−4.19	7	−4.01 to −4.34	−4.02
22	731910	1	10	7	Y	50	50	<−8.00;[d] −5.78 to −4.47	−4.92	45	−4.94 to −4.13	−4.4	26	−4.38 to −4.01	−4.11
23	733597	13	99	30	Y	56	56	−4.87 to −4.56	−4.73	54	−4.55 to −4.13	−4.42	44	−4.26 to −4.04	−4.14
24	729854	34	92	104	*N*						Inactive				

[a] The results for each compound are reported as the growth percent of treated cells when compared to untreated control cells accordingly for the following human tumor cell lines: (A) NCI-H460 (lung cancer); (B) SF-268 (CNS cancer), and (C) MCF7 (breast cancer).

[b] Active compounds have been selected for 60 cell lines assay.

[c] *N*, number of human tumor cell lines tested at the second stage assay. *N*1, *N*2, and *N*3, number of cell lines sensitive to this compound ($\log GI_{50} < -4.00$).

[d] Cell line RXF 393 (renal cancer) showed exceptional strong sensitivity to compound **17** (729725)—GI_{50} less than 0.01 μM, as well as cell line NCI/ADR-RES (breast cancer) has been exceptionally sensitive to compound **22** (731910)—GI_{50} less than 0.01 μM; the rest values of $\log GI_{50}$ are in mentioned ranges.

growth inhibitor for leukemia ($mean_{Leuk}$ $GI_{50} = -5.0$) and breast ($mean_{Breast}$ $GI_{50} = -5.38$) cancer cell lines. The above mean values of $\log GI_{50}$ for certain disease subpanels are compared with general MG_MID (averaged activity parameter $\log GI_{50}$ over all cell lines) for selected compounds in Figure 3.

A SAR study revealed that the presence of bulky substituents at the 9-position or methoxy-groups on aryl substituents improves the potency of the compounds. Compounds **21** and **22** with 4-benzyloxy-3-methoxyphenyl- and 5-(2′,5′-dichlorophenyl)-furan-2-yl-substituents at the 9-position are highly active, unlike compound **24** with 3-methoxy-4-hydroxyphenyl-substituent. Furthermore, individual cell lines have a differential sensitivity toward the tested compounds, with the highest sensitivity shown in Table 2.

4. COMPARE analysis

We have performed COMPARE analyses for all the active compounds in order to investigate the similarity of their cytotoxicity pattern (mean graph fingerprints) with those of known anticancer standard agents, NCI active synthetic compounds and natural extracts, which are present in public available databases.[27–29] Such analysis is based on comparing the patterns of differential growth inhibition for cultured cell lines and can potentially gain insight into the mechanism of the cytotoxic action. If the data pattern correlates well with that of compounds belonging to a standard agent database (Pearson's correlation coefficient (PCC) >0.6), the compound of interest may have the same mechanism of action. On the other hand, if the activity pattern does not correlate with any standard agent, it is possible that the compound has a novel mechanism of action. Standard COMPARE analyses were performed at the GI_{50} level. Compound **21** gave high correlations with stilbene analogs combretastatin A4 (NSC S645646; PCC = 0.838) and trimethoxy-4′-methyl-stilbene (NSC S638485; PCC = 0.705), which have an antimitotic mechanism via the inhibition of tubulin polymerization. Compound **22** also gave a correlation with a stilbene analog (NSC S603443; PCC = 0.719). We therefore assume that derivatives **21** and **22** interact with tubulin, but this only provides limited information regarding the mechanism of action, because other antitubulin agents did not correlate well with all the tested compounds. Since no other correlations with standard antitumor agents were found in the database, this could indicate a novel mechanism of action for 3,5,6,7-tetrahydro-2*H*-thiopyrano[2,3-*d*][1,3]thiazol-2-ones with a norbornane moiety, as well as prompted us to account tubulin as potential anticancer target for further investigations.

5. Lipophilicity studies

The lipophilicity is a well-known physico-chemical factor affecting biological activities, characterizing the distribution process of compound in the human organism and being a key factor of pharmacokinetic and

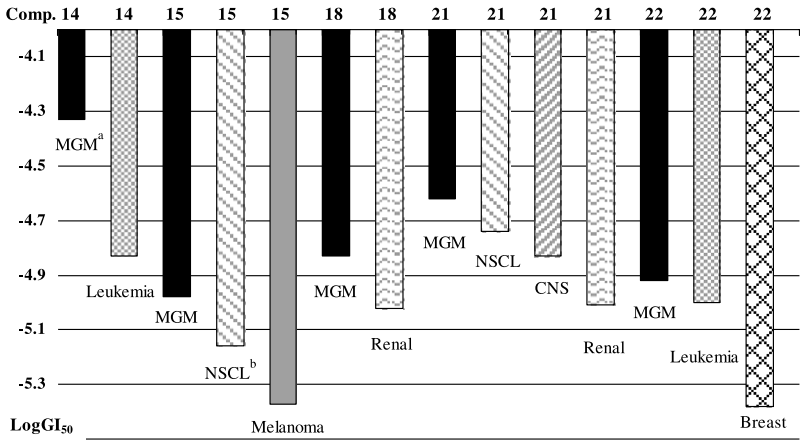

Figure 3. Selectivity of antitumor activity for some tested compounds [a]MGM—mean graph midpoints of $\log GI_{50}$ values—bars are colored in black and compared with average values for decease subpanels, whose bars are differently shaded. [b]NSCL—non-small cell lung cancer.

Table 2. The most sensitive to the synthesized compounds the individual tumor cell lines

Compound	Disease	Cell line	$\log GI_{50}$	$\log TGI$
14	Leukemia	MOLT-4	−5.16	−4.31
	Leukemia	RPMI-8226	−5.59	−5.01
15	Leukemia	RPMI-8226	−5.71	−4.31
	NSC lung cancer	NCI-H522	−7.54	−4.74
	Colon cancer	HCT-116	−5.57	−4.70
	Melanoma	M-14	−6.18	−4.83
	Melanoma	SK-MEL-2	−7.01	−5.32
	Ovarian cancer	IGROVI	−5.68	−4.68
	Renal cancer	RXF-393	−5.94	−4.68
	Renal cancer	UO-31	−5.51	−4.68
17	Renal cancer	RXF-393	<−8.00	−4.26
18	NSC lung cancer	NCI-H322M	−5.14	−4.67
	Colon cancer	KM12	−5.00	−4.65
	Renal cancer	RXF-393	−6.05	−4.55
	Renal cancer	ACHN	−4.98	−4.64
	Breast cancer	NCI/ADR-RES	−5.05	−4.68
21	Melanoma	LOX IMVI	−5.15	>−4.00
	Renal cancer	RXF-393	−5.24	>−4.00
	Renal cancer	TK-10	<−8.00	−5.09
	Renal cancer	ACHN	−5.49	−4.89
	Breast cancer	MDA-MB-231/ATCC	−5.19	−4.53
	CNS cancer	U251	−5.51	−4.96
22	Leukemia	MOLT-4	−5.40	−4.55
	Leukemia	SR	−5.04	>−4.00
	NSC lung cancer	NCI-H322M	−5.30	−4.67
	NSC lung cancer	NCI-H460	−5.33	−4.38
	Colon cancer	KM12	−5.36	−4.70
	Breast cancer	NCI/ADR-RES	<−8.00	−4.72
	Breast cancer	MCF7	−5.22	−4.56
	Breast cancer	T-47D	−5.78	−4.94

pharmacodynamic properties of drug molecules (plasma protein binding, blood–brain barrier (BBB) penetration, and penetration through cell membranes).[30] The anticancer activity in the in vitro assays prompted us to investigate the lipophilicity of the synthesized compounds. According to our design, the increased lipophilicity of these thiopyrano[2,3-*d*][1,3]thiazol-2-one derivatives should facilitate diffusion through biomembranes, thus enhancing cytostatic effectiveness. The presence of substituted heterocycles, as well as the conjunction of different rings in the molecule, may lead to unpredictable partitioning behavior. We have therefore employed a reversed-phase thin-layer chromatography (RP-TLC) as an alternative method for determining the lipophilicity,[31,32] and the results were compared with calculated values of $\log P$ (logarithm of partitioning coefficient of compound in phases *n*-octanol/water) for the QSAR studies. As shown below, a linear relationship

is found between the chromatographic lipophilicity parameter R_{m0} and $\log P$.

R_f values for the compounds were determined using RP-18 (Merck) TLC aluminum sheets as the stationary phase, and mobile phases were mixtures of acetone and water (acetone concentrations in the 65–85% range). The obtained R_f values were used for calculating the corresponding R_m values according to Eq. 1

$$R_m = log\left(\frac{1}{R_f} - 1\right). \quad (1)$$

The R_m values were extrapolated to zero acetone concentration by linear regression $R_m = A * C_{acetone} + R_{m0}$ ($R^2 = 0.9766$–0.9998) yielding R_{m0} values, which experimentally characterize the lipophilicity of the compounds (Table 2s, Supplementary data).

Regression analysis of the $\log P$ values, calculated by different computer programs ChemDraw (CambridgeSoft), Pallas 3.0 Demo (CompuDrug) and chromatographic R_{m0} values gives satisfactory linear models shown in Table 3. The ChemDraw ($C\log P$ algorithm) calculated $\log P$ values were found to correlate the best with the experimental RP-TLC results (Table 3) and were used in subsequent QSAR analysis.

The lipophilicity study showed that most of compounds possess optimum lipophilicities ($\log P \sim 2$–5) required for oral absorption and biomembrane penetration, even for BBB penetration. This bioavailability feature makes it possible to use these compounds in treatment of different cancer types including CNS cancer. It is interesting that the lipophilicities of the most active compounds **21** and **22** appear to be too high according to Lipinski's drug-likeness 'rules of five',[33] and this could cause insufficient biomembrane permeability of these active compounds in the organism. Clearly the lipophilicity has an influence on the activity, but it does not solely determine the cytotoxic activity of these compounds.

6. Docking studies

In order to elucidate possible mechanisms for the anticancer activity, we have performed docking studies using the Glide[34] (Schrodinger LLC.) and Fred[35] (Openeye Inc.) programs. The relevant stereoisomers of the compounds (according to the X-ray structure) were minimized with the MMFF force field in the MacroModel[34] package. In order to improve the electrostatic interactions modeling, we derived electrostatic potential (ESP) charges by the CHelp method[36] at the HF/6-31G* level of theory for each compound.[37] The derived partial charges were assigned to the structures and the geometries reoptimized with the MMFF force field. Docking was carried out against proteins reported as possible anticancer targets of thiazolidine derivatives: PPAR-γ receptor (PDB codes 1FM6 and 1NYX); Bcl-X_L–BH_3 peptides complex (PDB code: 1BXL) and tubulin (PDB code: 1SA1). Tubulin protein was chosen as one possible target for docking, because of the indirect pointers from the COMPARE analysis, and because of a relatively high Tanimoto (2D-structure fingerprint) similarity index[39,40] of tubulin ligand podophilotoxine with synthesized compounds. Selected target proteins were retrieved from PDB (<www.rcsb.org/pdb/>). For docking in Glide, they were prepared by Macromodel, *pprep* and *impref* utilities, included in the Schrödinger package. Docking yielded docking functions scores for target molecules.

7. QSAR modeling

A QSAR modeling seeks to uncover correlation of anticancer cytotoxicity with molecular descriptors and docking functions scores via multilinear models of the form 2, where x_i indicates a molecular descriptor:

$$\text{activity} = \sum_i x_i \alpha_i + b. \quad (2)$$

As dependent variables were chosen the mean graph midpoints of $\log GI_{50}$ parameter (MG_MID), $\log GI_{50}$ values for each cell line, and mean values of $\log GI_{50}$ for each cancer type cell lines subpanel. For the inactive compound the $\log GI_{50}$ value was assumed as the maximum concentration tested.

Mono-variable regression analysis gave correlation coefficients $r^2 \sim 0.6$–0.8 for the correlation of docking scores with $\log GI_{50}$ activity parameter, mainly for docking with PPARγ-receptor's and Bcl-X_L protein's binding sites. In order to further improve the predictive value, we decided to include other molecular descriptors. The independent variables used for the final QSAR studies are given in Table 4. All descriptors have been mean-centered prior to the analysis, and the value of the "*b*" coefficient in the regression equation therefore becomes equal to 0.

Multivariable regression analysis was performed using the partial least squares[41,42] method and simulated annealing for selecting models with a limited number of variables in order to provide better statistical models. The quality of the models is quantified by the correlation coefficient, r^2, the standard deviation, s, the Fisher's statistic, F, and the leave-one-out cross-validation correlation coefficient, q^2. For the QSAR multivariate models, the following limitations were imposed:

Table 3. Linear correlation of experimental R_{m0} (RP-TLC) and calculated $\log P$ ($C\log P$) values ($N = 11$)

Program	Model ($C\log P = a * R_{m0} + b$)	R^2	s	F
ChemDraw	$y = 1.1147x - 0.0305$	0.78	0.33	31.43
ChemDraw ($C\log P$ algorithm)	$y = 1.7323x - 1.0911$	0.90	0.32	80.98
Pallas 3.0 Demo	$y = 1.7332x - 1.6294$	0.88	0.33	68.76

Table 4. Molecular descriptors used for QSAR analysis

Descriptor code	Description	Ref.
GS	GlideScore—docking function score from Glide program	34
EM	E-model—docking function score from Glide program	34
SG	Shapegauss (represents all the atoms as smooth Gaussian functions)—docking function score from Fred program	35
CG	ChemGauss (combines Shapegaussian function with additional potentials between chemically complimentary groups)—docking function score from Fred program	35
PLP	PLP (piecewise linear potential)—docking function score from Fred program	35
CS	ChemScore (includes interaction between lipophilic atoms, hydrogen bond donors and acceptors, hydrogen bond acceptors and metals)—docking function score from Fred program	35
ZB	Zapbind (combination of surface area contact term and electrostatic interaction, both calculated using the Poisson–Boltzmann solvent approximation)—docking function score from Fred program	35
MW	Molecular weight	
$\log P$	logarithm of partitioning coefficient (calculated by C$\log P$ method)	38
TPSA	Topological polar surface area, calculated by Jchem package (ChemAxon), using P. Ertl algorithm	39
HOMO and LUMO	Energies of the highest occupied and the lowest unoccupied molecular orbitals (HF/6-31G*)	37
μ	Dipole moment (HF/6-31G*)	37
q_{min} and q_{max}	Minimal and maximal ESP charges, derived by CHELP algorithm (HF/6-31G*)	36, 37

Table 5. QSAR models derived by PLS regression analysis combined with simulated annealing

Cancer type/cell line of $\log GI_{50} - Y$ dependent variable	Compound	Regression equations	Number of variables	N	r^2	s	F	q^2
Breast cancer/T-47D	**1a**	$Y = 34.787 * \text{LUMO} + 0.002 * \text{ZB}$ (tubuline)	2	11	0.91	0.13	43	0.82
Breast cancer/T-47D	**1b**	$Y = 33.726 * \text{LUMO} - 0.042 * \text{CS}$ (1BLX)	2	11	0.91	0.13	40	0.83
Breast cancer/T-47D	**1c**	$Y = 35.259 * \text{LUMO} - 0.015 * \text{PLP}$ (1BLX) $- 0.029 * \text{CS}$ (1BLX)	3	11	0.93	0.11	33	0.88
Breast cancer/T-47D	**1d**	$Y = 33.826 * \text{LUMO} + 0.023 * \text{ZB}$ (1BLX) $- 0.025 * \text{PLP}$ (1BLX)	3	11	0.93	0.11	32	0.87
CNS cancer/SNB-19	**2**	$Y = -0.388 * \log P - 5.008 * q_{min} - 0.035 * \text{PLP}$ (1BLX)	3	11	0.91	0.09	24	0.84
Renal cancer/RFX 393	**3**	$Y = 52.288 * \text{LUMO} - 0.408 * \mu - 1.173 * \text{GS}$ (1FM6)	3	10	0.92	0.32	24	0.81
Colon cancer/HCT-116	**4**	$Y = 0.611 * \mu - 2.294 * q_{min} + 0.046 * \text{CS}$ (1FM6)	3	10	0.93	0.07	32	0.81

(1) Up to two docking scores (derived by the same program).
(2) A maximum of three variables.
(3) A minimum of 10 data points in the training subset.
(4) Correlation coefficients $r^2 > 0.9$ and $q^2 > 0.8$.

The models derived within these limitations are shown in Table 5, and they indicate that the cytotoxicity correlates well with the energy of the LUMO, corresponding to an electron-accepting ability. The mechanism of action of the compounds cannot be rationalized from the results of the docking studies, because the most efficient models **1a** and **1b** have almost equal impact of the scoring functions from dockings to tubulin and Bcl-X_L binding. Nevertheless, tubulin and Bcl-X_L should be used as potential targets for further rational structure design of anticancer thiopyrano[2,3-*d*][1,3]thiazol-2-ones and structure modification of obtained hit-compounds.

8. Conclusions

A set of novel fused thiopyrano[2,3-*d*]thiazol-2-one derivatives have been synthesized and ten of them displayed cytotoxicity against tumor cell lines with selectivity concerning lung, renal, breast, leukemia, and melanoma cancer types. Lipophilicity parameters, which are important for cell membrane penetration as well as blood–brain barrier penetration of potential drug, have been studied experimentally by RP-TLC and correlated with calculated $\log P$ values. These studies revealed that most of compounds possess optimum lipophilicities according to Lipinski rules, however the most active compounds **21** and **22** possess too high lipophilicity and could cause insufficient biomembrane permeability. The docking studies of the compounds with selected anticancer targets (PPAR-γ receptor, Bcl-X_L–BH_3 peptides complex and tubulin) resulted in a set of QSAR models with satisfactory statistical significance and predictive ability. The results obtained in these preliminary studies will be pursued for improving of anticancer potency and selectivity and development of new hit- and lead-compounds with the thiopyrano[2,3-*d*]thiazole scaffold via rational design and structure optimization.

9. Experimental

9.1. Materials and methods

All starting materials were purchased from Merck, Sigma–Aldrich or Lancaster and used without purification. Melting points are uncorrected and were measured in open capillary tubes on a Thomas-Hoover melting point apparatus. The IR spectra were recorded on 1600 FTIR Perkin-Elmer spectrometer as potassium bromide pallets and frequencies are expressed in cm^{-1}. The ^1H NMR spectra were recorded on Varian Gemini

300 MHz and ^{13}C NMR spectra on Varian Gemini 75 Hz in DMSO-d_6 using tetramethylsilane (TMS) as an internal standard (chemical shifts values are reported in parts per million units, coupling constants (J) are in hertz). Abbreviations are as follows: s, singlet; d, doublet; dd, double doublet; t, triplet; m, multiplet; and br, broad. The elemental analyses (C, H, and N) were performed at the Perkin-Elmer 2400 CHN and Carlo-Erba 1106 CHN analyzer and were within ±0.4% of the theoretical values. LC/MS were obtained on Agilent 1100 instrument.

The starting compounds: 2,4-thiazolidinedione (**1**),[43] 4-thioxo-2-thiazolidone (**2**)[13] were obtained according to methods described previously. 5-Ylidene-4-thioxo-2-thiazolidones (**3**–**13**) were prepared by treating 4-thioxo-thiazolidine-2-one with corresponding aldehydes R^1-CHO in glacial acetic acid at water bath (100 °C) 20 min, as described.[13,14]

9.2. Chemistry

9.2.1. General procedure for the preparation of 9-*R*-3,7-dithia-5-azatetracyclo[9.2.1.0^{2,10}.0^{4,8}]tetradecen-4(8)-ones-6 (14–24). A mixture of appropriate 5-*R*-methylidene-4-thioxo-2-thiazolidone (10 mmol) and norbornene-2 (11 mmol) was refluxed for 1 h with catalytic amount of hydroquinone (2–3 mg) for preventing of polymerization processes in 10 ml of glacial acetic acid, then left overnight at room temperature. The precipitated crystals were filtered off, washed with methanol (5–10 ml), and recrystallized from butanol (10–15 ml).

Substances **14**–**24** were isolated as white or yellowish powders. The NMR spectra show multiplets from the norbornane fragments in the 1.10–1.30 ppm region, signal from the CH group connected with the aromatic ring shows up as a doublet in the 3.36–3.98 region, which often overlays signals from the norbornane fragment.

9.2.2. 9-(4′-Chlorophenyl)-3,7-dithia-5-azatetracyclo-[9.2.1.0^{2,10}.0^{4,8}]tetradecen-4(8)-one-6 (14). Yield 89%, mp 222–224 °C. ^1H NMR (DMSO-d_6 + CCl_4) δ: 1.12m, 1.23m, 1.33m, 1.47m, 1.65m, 2.01m, 2.14m, 2.23m (9H, norbornane fragment), 3.37–3.43 (m, 2H, ArCH, SCH), 7.30d, 7.34d (4H, J = 8.6 Hz, 4-Cl-C_6H_4), 11.24 (s, 1H, NH). ^{13}C NMR (DMSO-d_6) δ: 28.29, 28.81, 34.03, 41.09, 42.97, 44.97, 51.15, 56.82, 113.23, 121.33, 128.50, 130.39, 132.00, 140.16, 170.34 (C=O). IR (KBr): 3446, 3126 (N–H), 2957(>C=C<), 2871 (CH_2), 1653 (C=O), 1579 (Ar), 1491, 1449, 1304, 1208, 1091, 1014, 922, 831, 681, 592 cm^{-1}. EI-MS: m/z 350 (97.5%, M^++1). Anal. ($C_{17}H_{16}ClNOS_2$) C, H, N.

9.2.3. 9-(4′-Methoxyphenyl)-3,7-dithia-5-azatetracyclo-[9.2.1.0^{2,10}.0^{4,8}]tetradecen-4(8)-one-6 (15). Yield 68%, mp 216–218 °C. ^1H NMR (DMSO-d_6 + CCl_4) δ: 1.12m, 1.22d, 1.33t, 1.47m, 1.65m, 2.02m, 2.12m, 2.23m, (9H, norbornane fragment), 3.29 (d, 1H, J = 10.7 Hz, SCH), 3.38 (d, 1H, J = 7.2 Hz, ArCH), 3.80 (s, 3H, OCH_3), 6.85d, 7.16d (4H, J = 8.8 Hz, 4-MeO–C_6H_4), 11.16 (s, 1H, NH). ^{13}C NMR (DMSO-d_6) δ: 28.40, 29.02, 34.07, 41.17, 43.02, 44.99, 51.36, 54.99, 57.25, 113.99, 114.58, 120.98, 129.61, 133.19, 158.43, 170.69 (C=O). IR (KBr) : 3449, 3151 (N–H), 2956 (C=C), 2870, 2831 (CH_2), 1659 (C=O), 1580, 1512 (Ar), 1437, 1301, 1253, 1206, 1176, 1036, 923, 832, 697, 609, 581 cm^{-1}. EI-MS: m/z 346 (100%, M^++1). Anal. ($C_{18}H_{19}NO_2S_2$) C, H, N.

9.2.4. 9-(4′-Methylphenyl)-3,7-dithia-5-azatetracyclo-[9.2.1.0^{2,10}.0^{4,8}]tetradecen-4(8)-one-6 (16). Yield 73%, mp 240–242 °C. ^1H NMR (DMSO-d_6) δ: 1.10m, 1.21d, 1.31t, 1.45m, 1.64m, 1.98d, 2.16m, 2.22m (9H, norbornane fragment), 3.32 (d, 1H, J = 10.4 Hz, SCH), 3.38 (d, 1H, J = 7.9 Hz, ArCH), 2.33 (s, 3H, CH_3), 7.12d, 7.17d (4H, J = 8.8 Hz, 4-Me–C_6H_4), 11.29 (s, 1H, NH). ^{13}C NMR (DMSO-d_6) δ: 20.61, 28.38, 29.01, 34.07, 41.16, 43.02, 45.46, 51.35, 57.15, 114.24, 121.14, 128.45, 129.24, 136.57, 138.25, 170.66 (C=O). IR (KBr) : 3424, 3122 (N–H), 2945 (C=C), 2870 (CH_2), 1649 (C=O), 1579, 1512 (Ar), 1446, 1300, 1206, 1113, 1039, 922, 821, 699, 606, 585 cm^{-1}. EI-MS: m/z 330 (98.2%, M^++1). Anal. ($C_{18}H_{19}NOS_2$) C, H, N.

9.2.5. 9-(4′-Hydroxyphenyl)-3,7-dithia-5-azatetracyclo-[9.2.1.0^{2,10}.0^{4,8}]tetradecen-4(8)-one-6 (17). Yield 69%, mp >260 °C. ^1H NMR (DMSO-d_6) δ: 1.11m, 1.18d, 1.31m, 1.47m, 1.64m, 2.04m, 2.13m, 2.21m (9H, norbornane fragment), 3.22 (d, 1H, J = 7.7 Hz, SCH), 3.35 (d, 1H, J = 10 Hz, ArCH), 6.70d, 7.03d (4H, J = 8.8 Hz, 4-HO–C_6H_4), 9.08 (s, 1H, OH), 11.29 (s, 1H, NH). ^{13}C NMR (DMSO-d_6) δ: 28.37, 29.01, 34.02, 41.14, 43.00, 45.04, 51.36, 57.20, 114.90, 115.33, 120.79, 129.50, 131.46, 156.50, 170.73 (C=O). IR (KBr) : 3420, 3129 (N–H, O–H), 2961 (C=C), 2873 (CH_2), 1636 (C=O), 1513 (Ar), 1447, 1369, 1304, 1249, 1228, 1110, 924, 834, 700, 646, 610 cm^{-1}. EI-MS: m/z 332 (100%, M^++1). Anal. ($C_{17}H_{17}NO_2S_2$) C, H, N.

9.2.6. 9-(2′-Chlorophenyl)-3,7-dithia-5-azatetracyclo-[9.2.1.0^{2,10}.0^{4,8}]tetradecen-4(8)-one-6 (18). Yield 72%, mp 259–261 °C. ^1H NMR (DMSO-d_6) δ: 1.14m, 1.23d, 1.35m, 1.45m, 1.62m, 1.95m, 2.10m, 2.24m (9H, norbornane fragment), 3.39 (m, 1H, SCH), 4.00 (d, 2H, J = 10.5 Hz, ArCH), 7.36m, 7.46d (4H, J = 8.6 Hz, 2-Cl–C_6H_4), 11.41 (s, 1H, NH). ^{13}C NMR (DMSO-d_6) δ: 28.25, 28.82, 34.19, 41.10, 41.69, 43.00, 51.21, 56.51, 112.54, 121.76, 127.78, 129.12, 129.48, 129.62, 133.39, 138.18, 170.30 (C=O). IR (KBr) : 3423, 3118 (N–H), 2961 (C=C), 2870 (CH_2), 1647 (C=O), 1577 (Ar), 1473, 1441, 1306, 1253, 1211, 1124, 1036, 951, 927, 759, 739, 690, 571 cm^{-1}. EI-MS: m/z 350 (100%, M^++1). Anal. ($C_{17}H_{16}ClNOS_2$) C, H, N.

9.2.7. 9-(Thiophen-2-yl)-3,7-dithia-5-azatetracyclo-[9.2.1.0^{2,10}.0^{4,8}]tetradecen-4(8)-one-6 (19). Yield 80%, mp 243–241 °C. ^1H NMR (DMSO-d_6) δ: 1.17m, 1.33m, 1.46m, 1.61m, 2.06m, 2.20m (10H, norbornane fragment), 3.43 (d, 1H, J = 7.2 Hz, SCH), 3.85 (d, 2H, J = 10.4 Hz, ArCH), 7.04m, 7.13d (J = 3.5 Hz), 7.48d (J = 5.5 Hz) (3H, thiophene), 11.49 (s, 1H, NH). ^{13}C NMR (DMSO-d_6) δ: 28.31, 28.99, 34.14, 40.79, 41.68, 43.00, 51.36, 58.24, 114.03, 121.17, 125.22, 127.04, 143.95, 170.56 (C=O). IR (KBr) : 3423, 3114 (N–H), 2947 (C=C), 2866 (CH_2), 1644 (C=O), 1584 (C=C,

thiophene), 1451, 1308, 1282, 1210, 1185, 1038, 926, 855, 787, 703, 624, 580 cm^{-1}. EI-MS: *m*/*z* 322 (100%, M^++1). Anal. ($C_{15}H_{15}NOS_3$) C, H, N.

9.2.8. 9-(3′,4′-Dimethoxyphenyl)-3,7-dithia-5-azatetracyclo[9.2.1.0^{2,10}.0^{4,8}]tetradecen-4(8)-one-6 (20). Yield 69%, mp 242–243 °C. ^{1}H NMR (DMSO-d_6) δ: 1.08m, 1.17d, 1.35t, 1.44m, 1.60m, 1.97ws, 2.06d, 2.22m (9H, norbornane fragment), 3.38–3.43 (m, 2H, SCH, ArCH), 3.76s, 3.78s (6H, 2*OCH_3), 6.89–7.01 (m, 3H, 3,4-$(OMe)_2$–C_6H_3), 11.45 (s, 1H, NH). ^{13}C NMR (DMSO-d_6) δ: 28.42, 29.04, 34.14, 41.24, 43.01, 45.42, 51.41, 55.41, 55.57, 57.14, 111.75, 112.41, 114.61, 120.57, 120.99, 133.70, 148.01, 148.66, 170.76 (C=O). IR (KBr) : 3450, 3121 (N–H), 2994, 2956 (C=C), 2872, 2835 (CH_2), 1649 (C=O), 1518 (Ar), 1467, 1421, 1291, 1259, 1238, 1142, 1024, 920, 815, 759, 703, 635, 564 cm^{-1}. EI-MS: *m*/*z* 376 (100%, M^++1). Anal. ($C_{19}H_{21}NO_3S_2$) C, H, N.

9.2.9. 9-(4′-Benzyloxy-3′-methoxyphenyl)-3,7-dithia-5-azatetracyclo[9.2.1.0^{2,10}.0^{4,8}]tetradecen-4(8)-one-6 (21). Yield 64%, mp 216–218 °C. ^{1}H NMR (DMSO-d_6) δ: 1.11m, 1.19d (J = 12.6 Hz), 1.32m, 1.45m, 1.65m, 2.03m, 2.14m, 2.21m, (9H, norbornane fragment), 3.29 (d, 1H, J = 10 Hz, SCH), 3.38 (d, 1H, J = 7.5 Hz, ArCH), 3.79 (s, 3H, OCH_3), 5.04 (s, 2H, CH_2), 6.81d (J = 8.1 Hz), 6.90s, 6.98d (J = 8.1 Hz) (3H, 3-OMe–4-BzO–C_6H_3), 7.38 (m, 5H, C_6H_5), 11.30s (s, 1H, NH). ^{13}C NMR (DMSO-d_6) δ: 28.40, 28.99, 34.13, 41.21, 42.98, 45.41, 51.39, 55.66, 57.05, 69.99, 112.73, 113.50, 114.52, 120.52, 120.99, 127.78, 128.31, 134.13, 137.10, 147.11, 149.01, 170.72 (C=O). IR (KBr) : 3423, 3115 (N–H), 2951 (C=C), 2871 (CH_2), 1642 (C=O), 1515 (Ar), 1452, 1418, 1379, 1261, 1218, 1140, 1015, 923, 853, 748, 697, 641, 621, 561 cm^{-1}. Anal. ($C_{25}H_{25}NO_3S_2$) C, H, N.

9.2.10. 9-[4-(2′,5′-Dichlorophenyl)-furan-2-yl]-3,7-dithia-5-azatetracyclo[9.2.1.0^{2,10}.0^{4,8}]tetradecen-4(8)-one-6 (22). Yield 60%, mp 198–200 °C. ^{1}H NMR (DMSO-d_6) δ: 1.27m, 1.38m, 1.54m, 1.66m, 2.08m, 2.18m, 2.35m (9H, norbornane fragment), 3.43 (d, 1H, J = 7.8 Hz, SCH), 3.67 (d, 1H, J = 10.4 Hz, ArCH), 6.56d (J = 3.3 Hz), 7.19d (J = 3.3 Hz) (2H, furane), 7.32d (J = 8.7 Hz), 7.53d (J = 8.7 Hz), 7.68s (3H, 2,5-diCl-C_6H_3), 11.44 (s, 1H, NH). ^{13}C NMR (DMSO-d_6) δ: 28.24, 28.85, 34.24, 41.81, 43.07, 51.29, 54.24, 110.25, 111.20, 112.93, 121.90, 126.56, 127.33, 128.30, 129.66, 132.20, 132.45, 147.46, 154.62, 170.52 (C=O). IR (KBr) : 3422, 3118 (N–H), 2952 (C=C), 2872 (CH_2), 1640 (C=O), 1583 (furan), 1537 (Ar), 1467, 1379, 1306, 1255, 1203, 1100, 925, 881, 812, 794, 698, 596, 569 cm^{-1}. Anal. ($C_{21}H_{17}Cl_2NO_2S_2$) C, H, N.

9.2.11. 9-(4′-Fluorophenyl)-3,7-dithia-5-azatetracyclo-[9.2.1.0^{2,10}.0^{4,8}]tetradecen-4(8)-one-6 (23). Yield 79%, mp 243–244 °C. ^{1}H NMR (DMSO-d_6) δ: 1.06m, 1.18d, 1.24–1.48m, 1.53–1.64m, 1.92d, 2.10m, 2.22m (9H, norbornane fragment), 3.42 (d, 1H, J = 7.8 Hz, ArCH), 3.48 (d, 1H, J = 10.2 Hz, SCH), 7.21d, 7.43d (4H, J = 8.9 Hz, 4-F–C_6H_4) 11.51 (s, 1H, NH). ^{13}C NMR (DMSO-d_6) δ: 28.40, 28.97, 34.12, 41.14, 43.02, 44.92, 51.28, 57.14, 113.80, 115.35 (d, 2C, J = 20.0 Hz, Ar), 121.26, 130.44 (d, 2C, J = 8.2 Hz, Ar), 137.42, 161.36 (d, J = 242.3 Hz, C–F), 170.52 (C=O). IR (KBr) : 3410, 3158, 3068 (N–H), 2952 (C=C), 2868 (CH_2), 1665 (C=O), 1509 (Ar), 1431, 1304, 1224, 1159, 1097, 1016, 924, 840, 687, 604, 567, 529 cm^{-1}. EI-MS: *m*/*z* 334 (100%, M^++1). Anal. ($C_{17}H_{16}FNOS_2$) C, H, N.

9.2.12. 9-(4′-Hydroxy-3′-methoxyphenyl)-3,7-dithia-5-azatetracyclo[9.2.1.0^{2,10}.0^{4,8}]tetradecen-4(8)-one-6 (24). Yield 74%, mp 267–269 °C; ^{1}H NMR (DMSO-d_6) δ: 1.13m, 1.20d, 1.32m, 1.47m, 1.66m, 2.09m, 2.13m, 2.23m (9H, norbornane fragment), 3.22 (d, 1H, J = 10.6 Hz, SCH), 3.35 (d, 1H, J = 7.3 Hz, ArCH), 3.83s (3H, OCH_3), 6.67d, 6.72d, 6.74s (3H, Ar), 8.54s (1H, OH), 11.14s (1H, NH). ^{13}C NMR (DMSO-d_6) δ: 28.43, 29.07, 34.15, 41.23, 43.02, 45.46, 51.45, 55.66, 57.19, 112.68, 114.94, 115.46, 120.87, 132.21, 145.76, 147.52, 170.82 (C=O). IR (KBr) : 3356w (N–H, OH), 2947 (C=C), 2866 (CH_2), 1653 (C=O), 1598, 1517 (Ar), 1453, 1431, 1359, 1267, 1206, 1150, 1120, 1028, 925, 853, 822, 780, 699, 641, 563 cm^{-1}. Anal. ($C_{18}H_{19}NO_3S_2$) C, H, N.

9.3. Crystal structure determination of 23

Crystal data: $C_{17}H_{16}FNOS_2$, triclinic, space group *P*-1, a = 9.6227(15), b = 9.6915(17), c = 9.8438(16) Å, α = 110.315(16)°, β = 113.377(15), γ = 92.527(13), V = 772.4(2) Å^3, Z = 2, T = 293(2) K.

Data collection: a colorless crystal of 0.50 × 0.33 × 0.07 mm was used to record 5570 (Cu Kα radiation, θ_{max} = 70.13°) intensities on a Kuma KM-4 diffractometer.[44] Accurate unit cell parameters were determined by least squares techniques from the θ values of 40 reflections, θ range 14.9–28.6°. The intensities were collected in the $\omega - 2\theta$ scan mode with graphite-monochromatized Cu Kα radiation. The intensities were corrected for Lorentz polarization effects and absorption using an empirical model derived from psi scans (μ(Cu Kα) = 3.225 mm^{-1}). The minimum and maximum transmissions were 0.368 and 0.678. The 2783 total unique reflections (R(int) = 0.0478) were used for further calculations.

Structure solution and refinement: the structure was solved by the direct methods using the program SHELXS-97,[45] and refinement was done against F^2 for all data using SHELXL-97.[45] The position of the H atom bonded to N atom was obtained from difference Fourier map and was refined freely. The remaining H atoms were positioned geometrically, and were refined with a riding model and with U_{iso} values constrained to be 1.2 times the U_{eq} value of the parent atom. The final refinement converged with R = 0.0498 (for 2548 data with $F^2 > 4\sigma(F^2)$), wR = 0.1439 (on F^2 for all data), and S = 1.041 (on F^2 for all data). The largest difference peak an hole were 0.496 and −0.318 e Å^{-3}. The molecular illustration was drawn using ORTEP-3 for Windows.[46] Software used to prepare material for publication was WINGX.[47]

The supplementary crystallographic data have been deposited at the Cambridge Crystallographic Data

Centre (CCDC), 12 Union ROAD, Cambridge CB2 1EZ, UK. Tel.: +44 1223 336 408; fax: +44 1223 336 033; e-mail: deposit@ccdc.cam.ac.uk, World Wide Web: http://www.ccdc.cam.ac.uk (Deposition No.: CCDC 278214).

9.4. In vitro anti-cancer screening

In vitro anti-cancer screening assays were performed according to NCI procedures.[24–26] The detailed method description is available as Supplementary data.

9.5. Lipophilicity studies (determination of R_m values)

For RP-TLC studies the aluminum chromatographic sheets (20 × 20 cm) RP-18 F_{254s} (Merck) were used. For the chromatographic purposes, different concentrations of acetone and water were chosen as optimal solvent system: 65%, 70%, 75%, 80%, and 85% (v/v) of acetone, respectively. Solutions of the tested compounds **14**–**24** in DMF (2 mg/ml) were spotted at 1.5 cm intervals and then the plates were eluted in chromatographic chambers, previously saturated with the solvent mixtures for 1 h. The plates were air-dried and the spots were visualized in UV-light at 254 nm. Triplicate TLC assays for each of 11 substances were carried out for ensuring reproducibility of the results and the mean R_f values were calculated for each substance/acetone concentration and transferred into corresponding R_m values. Monovariate regressions and their statistics were calculated at Microsoft Excel 2003.

Acknowledgments

We thank Dr. V. L. Narayanan from Drug Synthesis and Chemistry Branch, National Cancer Institute, Bethesda, MD, USA, for in vitro evaluation of anticancer activity. This work has been partially supported by the Sixth Framework Programme Marie Curie Host Fellowships for Early Stage Research Training under contract number MEST-CT-2004-504018 at University of Southern Denmark (SDU, Odense, Denmark) and Queen Jadwiga Fund Scholarship at Collegium Medicum of Jagellonian University (Krakow, Poland). This work was partially supported by grants from the Danish Center for Scientific Computing.

Supplementary data

Supplementary data associated with this article can be found, in the online version, at doi:10.1016/j.bmc.2006.03.053.

References and notes

1. Negwer, M. In *Organic-Chemical Drugs and Their Synonyms (An International Survey)/By Martin Negwer*, 7th ed.; Akademie: Berlin, 1994; Vols. 1–4.
2. Lesyk, R. B.; Zimenkovsky, B. S. *Curr. Org. Chem.* **2004**, *8*, 1547.
3. Degterev, A.; Lugovskoy, A.; Cardone, M.; Mulley, B.; Wagner, G.; Mitchison, T.; Yuan, J. *Nat. Cell Biol.* **2001**, *3*, 173.
4. Liu, W.; Bulgaru, A.; Haigentz, M.; Stein, C. A.; Perez-Soler, R.; Mani, S. *Curr. Med. Chem.: Anti-Cancer Agents* **2003**, *3*, 217.
5. Lugovskoy, A. A.; Degterev, A. I.; Fahmy, A. F.; Zhou, P.; Gross, J. D.; Yuan, J.; Wagner, G. *J. Am. Chem. Soc.* **2002**, *124*, 1234.
6. Carter, P. H.; Scherle, P. A.; Muckelbauer, J. A.; Voss, M. E.; Liu, R.-Q.; Thompson, L. A.; Tebben, A. J.; Solomon, K. A.; Lo, Y. C.; Li, Z.; Strzemienski, P.; Yang, G.; Falahatpisheh, N.; Xu, M.; Wu, Z.; Wu, Z.; Farrow, N. A.; Ramnarayan, K.; Wang, J.; Rideout, D.; Yalamoori, V.; Domaille, P.; Underwood, D. J.; Trzaskos, J. M.; Friedman, S. M.; Newton, R. C.; Decicco, C. P. *Proc. Natl. Acad. Sci. U.S.A.* **2001**, *98*, 11879.
7. Chen, H.; Fan, Y.-H.; Natarajan, A.; Guo, Y.; Iyasere, J.; Harbinski, F.; Luus, L.; Christ, W.; Aktas, H.; Halperin, J. A. *Bioorg. Med. Chem. Lett.* **2004**, *14*, 5401.
8. Theocharis, S.; Margeli, A.; Kouraklis, G. *Curr. Med. Chem.: Anti-Cancer Agents* **2003**, *3*, 239.
9. Debril, M.-B.; Renaud, J.-P.; Fajas, L.; Auwerx, J. *J. Mol. Med.* **2001**, *79*, 30.
10. Gelman, L.; Fruchart, J.-C.; Auwerx, J. *Cell. Mol. Life Sci.* **1999**, *55*, 932.
11. Farrow, B.; Evers, B. M. *Biochem. Biophys. Res. Commun.* **2003**, *301*, 50.
12. http://dtp.nci.nih.gov.
13. (a) Komaritsa, I. D.; Baranov, S. N.; Grishchuk, A. P. *Khimiya Geterotsiklicheskikh Soedinenii* **1967**, *4*, 664; (b) *Chem. Abstr.* **1968**, *68*, 49495; (c) Grishchuk, A. P.; Komaritsa, I. D.; Baranov, C. N. U.S.S.R. Patent SU 197594, 1967 (in Russian); (d) *Chem. Abstr.* **1968**, *68*, 36112.
14. Kassab, N. A. L.; Elnagdy, M. H.; Messeha, N. A.; Ead, H. A. R. *J. Pract. Chem.* **1972**, *314*, 799.
15. Kassab, N. A. L.; Abd-Allah, S. O.; Messeha, N. A. *J. Prakt. Chem./Chem-Ztg* **1974**, *316*, 209.
16. Kassab, N. A. L.; Messeha, N. A. *J. Pract. Chem.* **1973**, *315*, 1017.
17. Kassab, N. A. L.; Abd-Allah, S. O.; Abd-El-Razik, F. M. *Indian J. Chem., Sect. B* **1976**, *14*, 864.
18. Ead, H. A. R.; Kassab, N. A. L.; Koeppel, H.; Bloedorn, W.-D.; Schleinitz, K.-D. *J. Prakt. Chem./Chem-Ztg* **1980**, *322*, 155.
19. Ead, H. A. R.; Metwalli, N. H. *Egypt. J. Chem.* **1991**, *32*, 691.
20. Omar, M. T.; El-Aasar, N. K.; Saied, K. F. *J. Chem. Res. (M)* **2001**, *11*, 1127.
21. Abd-Allah, S. O.; Hamouda, H. A.; Ali, F. A. *Pharmazie* **1986**, *41*, 101.
22. Cremer, D.; Pople, J. A. *J. Am. Chem. Soc.* **1975**, *97*, 1354.
23. Wilson, A. J. C. In *International Tables for Crystallography*; Kluwer Academic: Dordrecht, 1992; Vol. C.
24. Monks, A.; Scudiero, D.; Skehan, P.; Shoemaker, R.; Paull, K.; Vistica, D.; Hose, C.; Langley, J.; Cronise, P.; Vaigro-Wolff, A. *J. Natl. Cancer Inst.* **1991**, *83*, 757.
25. Boyd, M. R.; Paull, K. D. *Drug Dev. Res.* **1995**, *34*, 91.
26. Boyd, M. R.. In *Cancer Drug Discovery and Development*; Teicher, B. A., Ed.; Humana Press, 1997; Vol. 2, pp 23–43.
27. Paull, K. D.; Shoemaker, R. H.; Hodes, L.; Monks, A.; Scudiero, D. A.; Rubinstein, L.; Plowman, J.; Boyd, M. R. *J. Natl. Cancer Inst.* **1989**, *81*, 1088.
28. (a) Paull, K. D.; Lin, C. M.; Malspeis, L.; Hamel, E. *Cancer Res.* **1992**, *52*, 3892; (b) http://dtp.nci.nih.gov/docs/compare/compare.html.
29. Zaharevitz, D. W.; Holbeck, S. L.; Bowerman, C.; Svetlik, P. A. *J. Mol. Graphics Modell.* **2002**, *20*, 297.

30. (a) Pliska, V.; Testa, B.; Van de Waterbeemd, H. In *Lipophilicity in Drug Action and Toxicology*; Pliska, V., Testa, B., Van de Waterbeemd, H., Eds.; VCH: Weinheim, 1996; pp 1–6; (b) Van de Waterbeemd, H.; Smith, D. A.; Beaumont, K.; Walker, D. K. *J. Med. Chem.* **2001**, *44*, 1313.
31. Mannhold, R.; Dross, K.; Sonntag, Ch. In *Lipophilicity in Drug Action and Toxicology*; Pliska, V., Testa, B., Van de Waterbeemd, H., Eds.; VCH: Weinheim, 1996; pp 141–156.
32. Dross, K.; Rekker, R. F.; de Vries, G.; Mannhold, R. *Quant. Struct.-Act. Relat.* **1999**, *18*, 549.
33. Lipinski, C. A.; Lombardo, L.; Dominy, B. W.; Feeney, P. J. *Adv. Drug Delivery Rev.* **2001**, *46*, 3.
34. (a) Maestro®, Macromodel, Glide, Schrodinger L.L.C; (b) Friesner, R. A.; Banks, J. L.; Murphy, R. B.; Halgren, T. A.; Klicic, J. J.; Mainz, D. T.; Repasky, M. P.; Knoll, E. H.; Shelley, M.; Perry, J. K.; Shaw, D. E.; Perry, F.; Penkin, P. S. *J. Med. Chem.* **2004**, *47*, 1739.
35. Omega®, Fred, OpenEye Scientific Software, 3600 Cerrillos Rd., Suite 1107, Santa Fe, NM 87507, USA.
36. Chirlian, L. E.; Francl, M. M. *J. Comput. Chem.* **1987**, *8*, 894.
37. Gaussian®03, Gaussian, Inc., Carnegie Office Park, Building Six, Carnegie, PA 15106, USA.
38. ChemDraw® 6.0, CambridgeSoft Inc., 100 Cambridge-Park Drive, Cambridge, MA 02140, USA.
39. JChem®, ChemAxon, ChemAxon Ltd, Máramaros köz 3/a, Budapest 1037, Hungary.
40. Willet, P. *J. Chem. Inf. Comput. Sci.* **1998**, *38*, 983.
41. Rannar, S.; Lindgren, F.; Geladi, P.; Wold, S. *J. Chemom.* **1994**, *8*, 111.
42. http://dasher.wustl.edu/.
43. (a) Turkevych, N. M.; Vvedenskij, V. M.; Petlichnaya, L. P. *Ukr. Khim. Zh. (Russ. Ed.)* **1961**, *27*, 680; (b) *Chem. Abstr.* **1962**, *56*, 73455.
44. Kuma Diffraction 1996. Version 8.0.1. KM-4 Software User's Guide, Wrocław, Poland.
45. Sheldrick, G. M. SHELXS-97 and SHELXL-97. Release 97-2. University Göttingen, Germany, 1997.
46. Farrugia, L. J. *J. Appl. Crystallogr.* **1997**, *30*, 565.
47. Farrugia, L. J. *J. Appl. Crystallogr.* **1999**, *32*, 837.